

Statistical and dynamical parts of the cumulants of conserved charges in relativistic heavy ion collisions

Xue Pan,^{1,*} Fan Zhang,¹ Zhiming Li,¹ Lizhu Chen,² Mingmei Xu,¹ and Yuanfang Wu^{1,†}

¹*Key Laboratory of Quark and Lepton Physics (MOE) and Institute of Particle Physics, Central China Normal University, Wuhan 430079, China*

²*School of Physics and Optoelectronic Engineering, Nanjing University of Information Science and Technology, Nanjing 210044, China*
(Received 20 November 2013; published 15 January 2014)

Poisson-like statistical fluctuations, which are caused by the finite number of produced particles, are estimated for the cumulants of conserved charges, i.e., net baryon, net electric, and net strangeness. They turn out to be the same as those baselines derived from the hadron resonance gas model. The energy and centrality dependence of net-proton cumulants at the Relativistic Heavy-Ion Collider (RHIC) are demonstrated to be mainly caused by statistical fluctuations. By subtracting the statistical fluctuations, the dynamical kurtosis of net- and total-proton cumulants from two versions of a multi-phase transport model and the ultra-relativistic quantum molecular dynamics model at current RHIC collision energies are presented. It is found that the observed sign change of the dynamical kurtosis of the net-proton cumulant cannot be reproduced by these three transport models. There is no significant difference between the net- and total-proton kurtosis in model calculations, in contrast to the data at RHIC.

DOI: [10.1103/PhysRevC.89.014904](https://doi.org/10.1103/PhysRevC.89.014904)

PACS number(s): 25.75.Nq, 25.75.Gz

I. INTRODUCTION

The cumulants of conserved charges have been suggested as good probes of the quantum chromodynamics (QCD) phase boundary. They are experimentally accessible and theoretically calculable.

At finite temperature and baryon chemical potential, effective chiral models [1] and some lattice QCD calculations [2,3] have predicted the existence of the QCD critical point (CP). Since the higher order cumulants of conserved charges are more sensitive to the correlation length, they have been suggested as critical related measurements in heavy ion collisions [4–14].

At vanishing chemical potential, lattice QCD calculations at physical quark masses have shown that the chiral crossover transition appears as the remnants of the second-order phase transition belonging to the O(4) universality class [15–17]. This makes it possible to explore the temperature of the QCD phase transition by the associated singularities of the higher order cumulants of conserved charges [18–22].

Moreover, recent calculations of lattice QCD indicate that the freeze-out conditions in heavy ion collisions can be reliably determined by the ratios of the first three-order cumulants of net electric charge [23]. So the measurements of the cumulants of conserved charges are crucial in locating the QCD phase boundary.

Before one can understand the physics of measured cumulants, one should first determine the contributions of various noncritical effects, such as global conservation laws in a subsystem [24], initial size fluctuations [25,26], and experimental acceptance cuts [25,27]. In this paper, we focus on the contributions of Poisson-like statistical fluctuations, which are caused by the finite number of produced particles [28–30].

For an ideal thermodynamic system, the number of particles is infinite. The statistical fluctuations are small and negligible in comparison to the critical one. However, for heavy ion collisions at the Relativistic Heavy-Ion Collider (RHIC), the number of produced particles is not infinite. For example, at the top energy of RHIC, the mean of the net-proton number is less than 10 [31]. Therefore, the statistical fluctuations are not negligible.

The predictions of a multiphase transport (AMPT) model [32] have shown that the behavior of the net-proton cumulants is dominated by the statistical fluctuations at RHIC collision energies [33]. Here, the net-proton cumulants measured through experiment are further compared with corresponding statistical fluctuations directly. This shows clearly how the behavior of net-proton cumulants is dominated by the statistical fluctuations at nine centralities and three RHIC collision energies.

By subtracting the Poisson-like statistical fluctuations, the dynamical net-proton cumulants can be recommended [12,33]. From the calculation of a nonlinear σ model [12] and the arguments of universality near the critical point [34], the dynamical kurtosis of the net protons is negative when the critical point is approached from the high-temperature side.

The expected sign change has been observed in the corresponding experimental measurements at RHIC; i.e., the dynamical kurtosis of net protons varies from negative to positive when the centrality varies from central to peripheral collisions, and the collision energy goes from high to low [35]. In contrast, the dynamical kurtosis of total protons is positive at all collision energies and centralities. Whether the sign change of the dynamical kurtosis of net protons indicates the appearance of a critical point or is simply caused by noncritical effects or experimental cuts is still not clear. A parallel investigation from known conventional models is helpful.

The paper is organized as follows. In Sec. II, the statistical parts of the cumulants of three kinds of conserved charges (i.e., net baryon, net electric charge, and net strangeness)

*panxuepx@gmail.com

†wuyf@phy.ccnu.edu.cn

are derived. They turn out to be the same as the baselines derived from hadron resonance gas (HRG) model. Then the contributions of statistical fluctuations to the RHIC preliminary net-proton cumulants are estimated in Sec. III. We find that the energy and centrality dependencies of net-proton cumulants are dominated by the statistical fluctuations. In Sec. IV, by using the generators of the AMPT default model, the AMPT with string melting model [32], and the ultra-relativistic quantum molecular dynamics (UrQMD) model [36], the dynamical kurtosis of net and total protons at nine centralities and seven RHIC collision energies are presented, respectively. They are both positive, in contrast to the observed sign change of the dynamical kurtosis of net protons of STAR data, but inconsistent with the observed data of dynamical kurtosis of total protons. Finally, the summary and conclusions are given in Sec. V.

II. STATISTICAL PART OF THE CUMULANTS

As we know, the statistical fluctuations of finite number of particles are well presented by the Poisson distribution [28]. There are hadrons with baryon number 1, electric-charge 1 or 2, and strangeness 1, or 2, or 3, respectively. We start from the simplest case. Suppose the baryon (N_1^B) and the antibaryon (N_{-1}^B) numbers both follow the Poisson distribution. The net-baryon probability distribution ($N_B = N_1^B - N_{-1}^B$) is therefore the cross-correlation of two Poisson distributions, i.e.,

$$\begin{aligned} f(N_B; \langle N_1^B \rangle, \langle N_{-1}^B \rangle) &= \sum_{x=-\infty}^{\infty} f(N_B + x, \langle N_1^B \rangle) f(x, \langle N_{-1}^B \rangle) \\ &= e^{-((N_1^B) + (N_{-1}^B))} \sum_{x=-\infty}^{\infty} \frac{\langle N_1^B \rangle^{N_B+x} \langle N_{-1}^B \rangle^x}{x! (N_B + x)!} \\ &= e^{-((N_1^B) + (N_{-1}^B))} (\langle N_1^B \rangle / \langle N_{-1}^B \rangle)^{N_B/2} I_{N_B} (2\sqrt{\langle N_1^B \rangle \langle N_{-1}^B \rangle}), \end{aligned} \quad (1)$$

where $\langle N_1^B \rangle$ and $\langle N_{-1}^B \rangle$ are means of N_1^B and N_{-1}^B , respectively. $I_{N_B}(z)$ is the modified Bessel function of the first kind. It is a standard Skellam distribution [37], the same as that derived from the HRG model [38].

The net-baryon cumulants (κ_k^B) can be obtained by the cumulant-generating function (CGF),

$$K_B(t; \langle N_1^B \rangle, \langle N_{-1}^B \rangle) = \sum_{k=0}^{\infty} \frac{t^k}{k!} \kappa_k^B, \quad (2)$$

where $K_B(t; \langle N_1^B \rangle, \langle N_{-1}^B \rangle) = \ln G(e^t; \langle N_1^B \rangle, \langle N_{-1}^B \rangle)$, and $G(t; \langle N_1^B \rangle, \langle N_{-1}^B \rangle)$ is the probability-generating function (PGF) of the Skellam distribution, i.e.,

$$\begin{aligned} G(t; \langle N_1^B \rangle, \langle N_{-1}^B \rangle) &= \sum_{N_B=0}^{\infty} f(N_B; \langle N_1^B \rangle, \langle N_{-1}^B \rangle) t^{N_B} \\ &= G(t; \langle N_1^B \rangle) G(1/t; \langle N_{-1}^B \rangle) \\ &= e^{-((N_1^B) + (N_{-1}^B)) + (N_1^B)t + (N_{-1}^B)/t}. \end{aligned} \quad (3)$$

So the even- and odd-order net-baryon cumulants are

$$\begin{aligned} \kappa_{2k}^B &= \langle N_1^B \rangle + \langle N_{-1}^B \rangle, \\ \kappa_{2k+1}^B &= \langle N_1^B \rangle - \langle N_{-1}^B \rangle. \end{aligned} \quad (4)$$

They are uniquely determined by the means of baryon and antibaryon numbers.

For electric charged particles, there are four kinds of particles: a charge-one particle (N_1^Q) and its antiparticle (N_{-1}^Q) and a charge-two particle (N_2^Q) and its antiparticle (N_{-2}^Q). Suppose the multiplicity of each kind of particle follows the Poisson distribution and the net-charge probability distribution of charge-one particles ($N_{1Q} = N_1^Q - N_{-1}^Q$) is a Skellam distribution again, the same as Eq. (1). For charge-two particles, the probability distributions of charges ($2N_2^Q$) and anticharges ($2N_{-2}^Q$) do not follow a Poisson distribution but are

$$f(2N_2^Q; 2\langle N_2^Q \rangle) = \langle N_2^Q \rangle^{2N_2^Q} e^{-\langle N_2^Q \rangle} / N_2^Q! \quad (5)$$

and

$$f(2N_{-2}^Q; 2\langle N_{-2}^Q \rangle) = \langle N_{-2}^Q \rangle^{2N_{-2}^Q} e^{-\langle N_{-2}^Q \rangle} / N_{-2}^Q!, \quad (6)$$

respectively. The probability distribution of the net charge of charge-two particles ($2N_{2Q} = 2N_2^Q - 2N_{-2}^Q$) is their cross-correlation,

$$\begin{aligned} f(2N_{2Q}; 2\langle N_2^Q \rangle, 2\langle N_{-2}^Q \rangle) &= \sum_{x=-\infty}^{\infty} f(2N_{2Q} + x, \langle N_2^Q \rangle) f(x, \langle N_{-2}^Q \rangle) \\ &= e^{-((N_2^Q) + (N_{-2}^Q))} \sum_{x=-\infty}^{\infty} \frac{\langle N_2^Q \rangle^{2N_{2Q}+x} \langle N_{-2}^Q \rangle^x}{x! (2N_{2Q} + x)!}. \end{aligned} \quad (7)$$

So, the probability distribution of the net charge of all charged particles ($N_Q = N_{1Q} + 2N_{2Q}$) is the convolution of the probability distributions of the net charges of charge-one and charge-two particles, i.e.,

$$\begin{aligned} f(N_Q; \langle N_1^Q \rangle, \langle N_{-1}^Q \rangle, 2\langle N_2^Q \rangle, 2\langle N_{-2}^Q \rangle) &= \sum_{x=-\infty}^{\infty} f(x; \langle N_1^Q \rangle, \langle N_{-1}^Q \rangle) f(N_Q - x; 2\langle N_2^Q \rangle, 2\langle N_{-2}^Q \rangle) \\ &= \sum_{x=-\infty}^{\infty} e^{-((N_1^Q) + (N_{-1}^Q))} \sum_{n=-\infty}^{\infty} \frac{\langle N_1^Q \rangle^{x+n} \langle N_{-1}^Q \rangle^n}{n! (x+n)!} \\ &\quad \times e^{-((N_2^Q) + (N_{-2}^Q))} \sum_{m=-\infty}^{\infty} \frac{\langle N_2^Q \rangle^{(N_Q-x)/2+m} \langle N_{-2}^Q \rangle^m}{m! [(N_Q-x)/2+m]!}. \end{aligned} \quad (8)$$

From its CGF and PGF, the even- and odd-order cumulants of net charge can be derived easily:

$$\begin{aligned} \kappa_{2k}^Q &= \langle N_1^Q \rangle + \langle N_{-1}^Q \rangle + 2^{2k} (\langle N_2^Q \rangle + \langle N_{-2}^Q \rangle), \\ \kappa_{2k+1}^Q &= \langle N_1^Q \rangle - \langle N_{-1}^Q \rangle + 2^{2k+1} (\langle N_2^Q \rangle - \langle N_{-2}^Q \rangle). \end{aligned} \quad (9)$$

They are also consistent with those obtained from the HRG model [38]. It should be noticed that the ratio κ_4^Q / κ_2^Q , i.e., the

product of kurtosis and variance, is

$$\frac{\kappa_4^Q}{\kappa_2^Q} = \kappa_4^Q \sigma_Q^2 = \frac{\langle N_1^Q \rangle + \langle N_{-1}^Q \rangle + 16(\langle N_2^Q \rangle + \langle N_{-2}^Q \rangle)}{\langle N_1^Q \rangle + \langle N_{-1}^Q \rangle + 4(\langle N_2^Q \rangle + \langle N_{-2}^Q \rangle)}. \quad (10)$$

It is not one, as in the case of net baryons or net protons [39], but determined by the means of the numbers of four kinds of charged particles.

For strangeness, there are six kinds of particles, i.e., strange-one, strange-two, and strange-three particles and their antiparticles. If the number of each kind of particle follows the Poisson distribution, similarly, the even- and odd-order net-strangeness cumulants can be derived as

$$\begin{aligned} \kappa_{2k}^S &= \langle N_1^S \rangle + \langle N_{-1}^S \rangle + 2^{2k}(\langle N_2^S \rangle + \langle N_{-2}^S \rangle) \\ &\quad + 3^{2k}(\langle N_3^S \rangle + \langle N_{-3}^S \rangle), \\ \kappa_{2k+1}^S &= \langle N_1^S \rangle - \langle N_{-1}^S \rangle + 2^{2k+1}(\langle N_2^S \rangle - \langle N_{-2}^S \rangle) \\ &\quad + 3^{2k+1}(\langle N_3^S \rangle - \langle N_{-3}^S \rangle). \end{aligned} \quad (11)$$

They are also the same as those obtained from the HRG model [38].

So starting from the assumption that all kinds of conserved charge particles and antiparticles are produced independently, or follow the Poisson distribution, the distributions and corresponding cumulants of the three kinds of net charges are derived. They turn out to be the same as those baselines obtained from the HRG model, where the Boltzmann approximation is implemented and the quantum effects of the electric-charged pion are neglected [38]. This shows that the baselines of the cumulants of conserved charges are in fact the fluctuations of independently produced particles, or pure Poisson-like statistical fluctuations. They are completely determined by the means of particle and antiparticle numbers.

III. STATISTICAL PART OF THE NET-PROTON CUMULANTS AT RHIC

The neutron is not detectable in experiments; however, the proton number fluctuations can reflect the singularity of baryon susceptibility very well [8]. Replacing the means of baryon and antibaryon number in Eq. (4) by means of proton ($\langle N_p \rangle$) and antiproton ($\langle N_{\bar{p}} \rangle$) numbers, the statistical net-proton cumulants can be obtained. They are the variance,

$$\sigma_{p,\text{stat}}^2 = \langle N_p \rangle + \langle N_{\bar{p}} \rangle, \quad (12)$$

the normalized cumulants, i.e., skewness and kurtosis,

$$S_{p,\text{stat}} = \frac{\langle N_p \rangle - \langle N_{\bar{p}} \rangle}{(\langle N_p \rangle + \langle N_{\bar{p}} \rangle)^{3/2}}, \quad \kappa_{p,\text{stat}} = \frac{1}{\langle N_p \rangle + \langle N_{\bar{p}} \rangle}, \quad (13)$$

and the ratios of the third- and fourth-order cumulants to the second one, i.e., the products of skewness and standard deviation and of kurtosis and variance,

$$S_{p,\text{stat}} \sigma_{p,\text{stat}} = \frac{\langle N_p \rangle - \langle N_{\bar{p}} \rangle}{\langle N_p \rangle + \langle N_{\bar{p}} \rangle}, \quad \kappa_{p,\text{stat}} \sigma_{p,\text{stat}}^2 = 1. \quad (14)$$

From these expressions, it is clear that except for $\kappa_{p,\text{stat}} \sigma_{p,\text{stat}}^2$ being a constant, all others are determined by the means of proton and antiproton numbers. As we know, with increasing

collision energy, and in more central collisions, the means of produced proton and antiproton numbers increase. The difference between the proton and antiproton means becomes less and less. So the statistical parts of the normalized cumulants and cumulant ratios decrease. In particular, $S_p \sigma_p$ decreases faster, and the skewness (S_p) decreases the fastest.

However, at lower collision energies, due to the baryon stopping effect [40], a large number of protons from initial nuclei remain in the formed system. This situation becomes more serious at even lower energies. For example, at 7.7 GeV, the lowest collision energy, the antiproton mean is two orders of magnitude smaller than that of the proton. In this case, all statistical cumulants from Eq. (4) are mainly determined by the proton mean. This is why all order cumulants are close to each other at lower collision energies (cf. Fig. 1 of Ref. [25] and Fig. 2 of Ref. [41]).

With increasing collision energy, the baryon stopping effect becomes weaker and weaker. At the higher energies, the contribution of the antiproton is not negligible. The statistical fluctuations of odd-order cumulants is the mean of net-proton number from Eq. (4), and they decrease rapidly with increasing energy. This is why the odd-order cumulants decrease together, and obviously separate from even-order ones with the increase of collision energy (cf. Fig. 1 of Ref. [25] and Fig. 2 of Ref. [41]).

From the means of proton and antiproton numbers at nine centralities and three RHIC collision energies, $\sqrt{s_{NN}} = 19.6, 62.4, \text{ and } 200 \text{ GeV}$ [31], the statistical standard deviation, skewness, and kurtosis of net protons are calculated. They are presented by open black circles in Fig. 1, where the solid red circles are the data. The three panels from left to right correspond to the three collision energies, respectively.

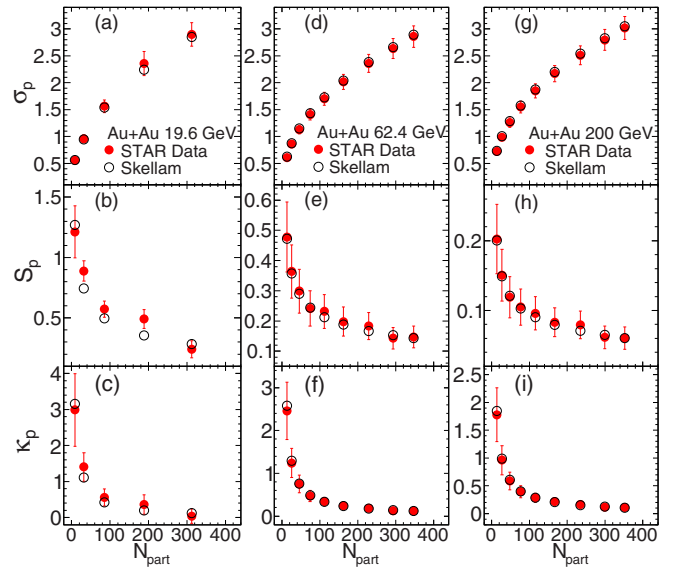


FIG. 1. (Color online) Centrality dependence of the statistical standard deviation (σ_p), skewness (S_p), and kurtosis (κ_p) of the net-proton distribution (open black circles) and corresponding experimental data (solid red circles) for Au + Au collisions at $\sqrt{s_{NN}} = 19.6 \text{ GeV}$ (left panels), 62.4 GeV (middle panels), and 200 GeV (right panels).

The figure shows that all statistical cumulants (open black circles) are close to corresponding data (solid red circles). The differences between them are one order of magnitude smaller. So the centrality and energy dependence of net-proton cumulants at RHIC are dominated by its statistical parts. As expected, the statistical skewness S_p is first and greatly suppressed when the collision energy increases from 19.6 to 200 GeV.

IV. DYNAMICAL KURTOSIS OF NET AND TOTAL PROTONS AT RHIC

In order to see the difference between directly measured cumulants and statistical ones, dynamical cumulants are recommended and defined as [30,33]

$$\kappa_{p,dyn} = \kappa_p - \kappa_{p,stat}. \quad (15)$$

These measure the correlations between charges. If the particles are produced independently, the dynamical cumulants are zero.

Calculations from lattice QCD have shown that near the critical temperature of the chiral phase transition, the kurtosis at $\mu_B = 0$ and $m_q = 0$ is positive. It could be negatively divergent near the critical point at nonvanishing chemical potential and physical mass [42]. The nonlinear σ model has demonstrated that if the critical point is approached from the high-temperature side, the dynamical kurtosis will change from negative to positive [12], although the negative values are very small. Calculations using the three-dimensional Ising model show a similar critical behavior [43], whereas calculations using the three-dimensional O(4) model show that the kurtosis oscillates between positive and negative. So the negative kurtosis is not specific to the critical end point (Ising universality). It may be associated with the chiral phase transition [O(4) universality] [21]. Anyway, the behavior of dynamical kurtosis at RHIC is highly interesting.

The dynamical kurtosis of net and total protons at nine centralities and seven RHIC beam energies ($\sqrt{s_{NN}} = 7.7, 11.5, 19.6, 27, 39, 62.4, \text{ and } 200$ GeV) are shown in Fig. 2(a) and 2(e), respectively [35]. Figure 2(a) shows clearly how the dynamical kurtosis of net protons varies with two controlling parameters, i.e., energy and centrality. It is negative at noncentral collisions and higher energies, i.e., $\sqrt{s_{NN}} > 19.6$ GeV, and positive at $\sqrt{s_{NN}} < 19.6$ GeV. The black solid circles for the most peripheral collisions highlight this change. The positive and negative values of the dynamical kurtosis of net protons indicate, respectively, that the peaks of net-proton distributions are sharper and flatter than those of the corresponding Skellam distributions.

The figure also shows that the values of dynamical kurtosis are not zero and are one order of magnitude smaller than that directly measured. This indicates that protons and antiprotons are not independently produced at RHIC.

In order to see whether the negative kurtosis can be caused by noncritical effects or by conventional particle production mechanisms, we calculate the dynamical kurtosis in the AMPT default model, the AMPT with string model [32], and the UrQMD model [36], where no critical behavior is implemented in these models. As we know, the initial size fluctuations are well taken into account in these three transport models by the Glauber model. However, the electric charge conservation of produced particles is not fully preserved in the AMPT models. The UrQMD model is better at taking the conservation of final state charges into account.

We simulate Au + Au collisions at seven corresponding collision energies by these three models. The calculations of dynamical net-proton cumulants are performed in the same way as the experimental analysis [31]. The centrality bins are selected by the multiplicity of charged particles except for protons and antiprotons within pseudo-rapidity window $|\eta| < 0.5$. The proton and antiproton measurements are carried out at the mid-rapidity window $|y| < 0.5$ in the

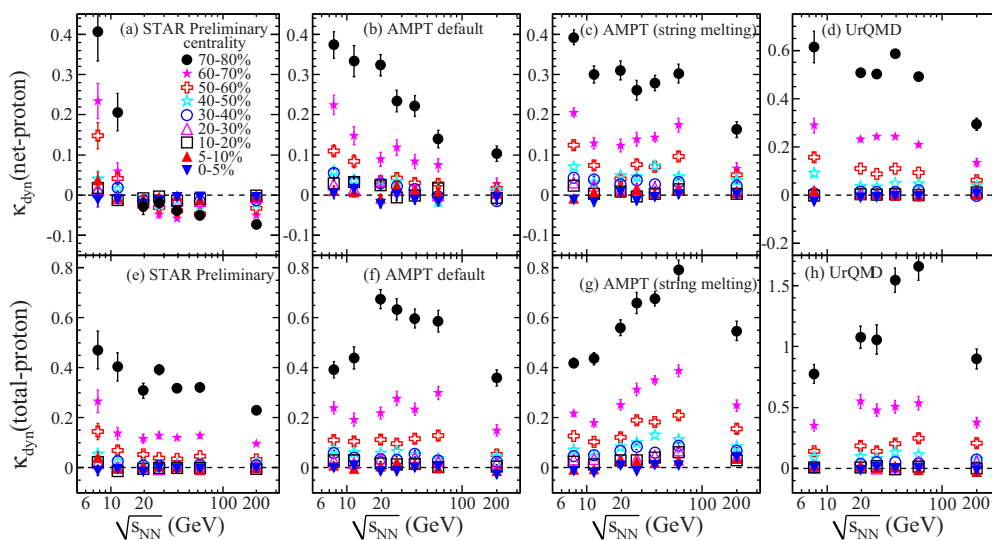


FIG. 2. (Color online) Energy dependence of the dynamical net-proton kurtosis (upper panels) and total-proton kurtosis (lower panels) at nine centralities for Au + Au collisions at RHIC. The results come from experimental data [(a) and (e)] [35], the AMPT default model [(b) and (f)], the AMPT with string melting model [(c) and (g)], and the UrQMD model [(d) and (h)], respectively.

transverse momentum range $0.4 < p_T < 0.8$ GeV/ c . The dynamical kurtosis of net and total protons in each centrality bin are estimated by the centrality bin width correction (CBWC) method [44]. They are presented in the upper and lower panels of Fig. 2, respectively, where the first column shows the data from RHIC/STAR and the second, third, and fourth columns are the results from the AMPT default, the AMPT with string melting, and the UrQMD models, respectively.

From Figs. 2(b), 2(c), and 2(d), it is clear that the dynamical kurtosis of net protons from the three model calculations are all positive at given centralities and energies, in contrast to the data in Fig. 2(a). So the conventional particle production mechanisms implemented in these three transport models cannot reproduce the observed sign change of the dynamical kurtosis of net protons. This inconsistency indicates that there should be additional correlations which have not been taken into account in these three transport models.

It is too early to draw a conclusion as to whether the related sign change is critical signal. Since the absolute value of negative kurtosis is very small (less than 0.1), if we change experimental cuts, such as the phase space windows of the analysis, the definition of centrality, and the centrality bin width corrections [26,44], the results may change accordingly. But, up to now, how to choose the experimental cuts and how to reduce the noncritical effects are still in progress.

On the other hand, the obtained results from the current theoretical calculations and experimental measurements are encouraging. The behavior of dynamical kurtosis is very interesting and worthy of further investigations.

From Figs. 2(f), 2(g), and 2(h), it is also clear that the dynamical kurtosis values of total protons from the three model calculations are all positive, which is inconsistent with the data, as shown in Fig. 2(e). They are all similar to those of dynamical kurtosis of net protons in the model calculations, as shown in Figs. 2(b), 2(c), and 2(d). So there is no significant difference between conserved and nonconserved charge in model calculations. However, the experimental data in Figs. 2(a) and 2(e) show that the behavior of conserved charge is quite different from that of nonconserved charge. This indicates again that some correlations between conserved charges are missed in these three transport models.

The quantitative difference between the two versions of the AMPT and the UrQMD models can be observed in the peripheral collisions, where the results from the UrQMD model are all much larger than those from the two versions of the AMPT model. This may be caused by a strict conservation of final-state charged particles in the UrQMD model, which leads to a stronger correlation between charged particles in peripheral collisions, where the number of produced particles are smaller than those of central collisions.

V. SUMMARY AND CONCLUSIONS

In this paper, we argue that, at RHIC collision energies, the Poisson-like statistical fluctuations in higher order cumulants of conserved charges are not negligible. Starting from independent particle production, i.e., assuming the Poisson distribution for the number of conserved charge particles, we derived the statistical cumulants of net baryons, net electric charge, and net strangeness. They are uniquely determined by the means of charged particle and antiparticle numbers and are the same as those baselines obtained from the HRG model. So the baselines of higher order cumulants of conserved charges are essentially the statistical fluctuations.

From the means of proton and antiproton numbers given by RHIC/STAR experiments, the statistical standard deviation, skewness, and kurtosis are estimated. They are close to the data at nine centralities and three RHIC collision energies. So the net-proton cumulants at RHIC are dominated by the statistical fluctuations.

By subtracting the statistical fluctuations, the dynamical kurtosis values of net and total protons from two versions of the AMPT model and the UrQMD model at RHIC collision energies are presented. It is found that the dynamical kurtosis of net protons is small, but not zero. This indicates that protons and antiprotons are not produced independently in these models, which is inconsistent with the data.

However, the observed sign change of the dynamical kurtosis of net protons at RHIC cannot be reproduced by conventional particle production mechanisms implemented in these three models. This inconsistency between the model calculations and experimental data indicates that there should be additional correlations between conserved charges in heavy ion collisions which have not been implemented into these three transport models.

In addition, model calculations show dynamical kurtosis values of total protons are all positive at observed centralities and energies, which is inconsistent with the data. There is no significant difference between the kurtosis of net and total protons or between conserved and nonconserved charges in the model calculations. However, from current experimental data, the centrality and energy dependence of dynamical kurtosis of net protons has a sign change, and the dynamical kurtosis of total protons stays positive. The behavior of dynamical kurtosis of net protons is significantly different from that of total protons. This shows again that some correlation effects in conserved charges are missing in these models.

ACKNOWLEDGMENTS

This work is supported in part by the Major State Basic Research Development Program of China under Grant No. 2014CB845402, the NSFC of China under Grants No. 10835005, No. 11221504, No. 11005046, and No. 11005045, and the Ministry of Education of China with Project No. 20120144110001.

[1] M. Asakawa and K. Yazaki, *Nucl. Phys. A* **504**, 668 (1989).

[2] Z. Fodor and S. D. Katz, *Phys. Lett. B* **534**, 87 (2002); *J. High Energy Phys.* 03 (2002) 014.

- [3] C. Schmidt, C. R. Allton, S. Ejiri, S. J. Hands, O. Kaczmarek, F. Karsch, and E. Laermann, *Nucl. Phys. B (Proc. Suppl.)* **119**, 517 (2003); R. V. Gavai, *Nucl. Phys. A* **862**, 104 (2011).
- [4] J. I. Kapusta and A. P. Vischer, and R. Venugopalan, *Phys. Rev. C* **51**, 901 (1995).
- [5] M. Stephanov, K. Rajagopal, and E. Shuryak, *Phys. Rev. Lett.* **81**, 4816 (1998).
- [6] S. Gavin, [arXiv:nucl-th/9908070](https://arxiv.org/abs/nucl-th/9908070); D. Bower and S. Gavin, *Phys. Rev. C* **64**, 051902 (2001).
- [7] K. Paeck, H. Stöcker, and A. Dumitru, *Phys. Rev. C* **68**, 044907 (2003).
- [8] Y. Hatta and M. A. Stephanov, *Phys. Rev. Lett.* **91**, 102003 (2003).
- [9] S. Ejiri, F. Karsch, and K. Redlich, *Phys. Lett. B* **633**, 275 (2006).
- [10] M. A. Stephanov, *Phys. Rev. Lett.* **102**, 032301 (2009).
- [11] Á. Mócsy and P. Sorensen, *Phys. Lett. B* **690**, 135 (2010).
- [12] M. A. Stephanov, *Phys. Rev. Lett.* **107**, 052301 (2011).
- [13] J. I. Kapusta and J. M. Torres-Rincon, *Phys. Rev. C* **86**, 054911 (2012).
- [14] J. Steinheimer and J. Randrup, *Phys. Rev. Lett.* **109**, 212301 (2012).
- [15] Y. Aoki, G. Endrődi, Z. Fodor, S. D. Katz, and K. K. Szabó, *Nature (London)* **443**, 675 (2006).
- [16] S. Ejiri, F. Karsch, E. Laermann, C. Miao, S. Mukherjee, P. Petreczky, C. Schmidt, W. Soeldner, and W. Unger, *Phys. Rev. D* **80**, 094505 (2009).
- [17] A. Bazavov *et al.* (HotQCD Collaboration), *Phys. Rev. D* **85**, 054503 (2012).
- [18] F. Karsch and K. Redlich, *Phys. Lett. B* **695**, 136 (2011); P. Braun-Munzinger, B. Friman, F. Karsch, K. Redlich, and V. Skokov, *Phys. Rev. C* **84**, 064911 (2011).
- [19] O. Kaczmarek, F. Karsch, E. Laermann, C. Miao, S. Mukherjee, P. Petreczky, C. Schmidt, W. Soeldner, and W. Unger, *Phys. Rev. D* **83**, 014504 (2011).
- [20] A. Bazavov *et al.* (HotQCD Collaboration), *Phys. Rev. D* **86**, 034509 (2012).
- [21] B. Friman, F. Karsch, K. Redlich, and V. Skokov, *Eur. Phys. J. C* **71**, 1694 (2011).
- [22] S. Borsányi, Z. Fodor, S. D. Katz, S. Krieg, C. Ratti, and K. Szabó, *J. High Energy Phys.* 01 (2012) 138.
- [23] S. Mukherjee and M. Wagner, [arXiv:1307.6255](https://arxiv.org/abs/1307.6255).
- [24] A. Bzdak, V. Koch, and V. Skokov, *Phys. Rev. C* **87**, 014901 (2013).
- [25] X. Luo (for the STAR Collaboration), *Nucl. Phys. A* **904-905**, 911c (2013).
- [26] L. Chen, Z. Li, and Y. Wu, [arXiv:1312.0749](https://arxiv.org/abs/1312.0749).
- [27] A. Bzdak and V. Koch, *Phys. Rev. C* **86**, 044904 (2012).
- [28] A. Bialas and R. Peschanski, *Nucl. Phys. B* **273**, 703 (1986); **308**, 857 (1988); *Phys. Lett. B* **207**, 59 (1988).
- [29] E. A. De Wolf, I. M. Dremin, and W. Kittel, *Phys. Rep.* **270**, 1 (1996); C. Athanasiou, K. Rajagopal, and M. Stephanov, *Phys. Rev. D* **82**, 074008 (2010).
- [30] C. Pruneau, S. Gavin, and S. Voloshin, *Phys. Rev. C* **66**, 044904 (2002); J. Adams *et al.* (STAR Collaboration), *ibid.* **68**, 044905 (2003); B. I. Abelev *et al.* (STAR Collaboration), *ibid.* **79**, 024906 (2009).
- [31] M. M. Aggarwal *et al.* (STAR Collaboration), *Phys. Rev. Lett.* **105**, 022302 (2010).
- [32] Z. W. Lin, C. M. Ko, B. A. Li, B. Zhang, and S. Pal, *Phys. Rev. C* **72**, 064901 (2005).
- [33] L. Chen, X. Pan, F. Xiong, L. Li, N. Li, Z. Li, G. Wang, and Y. Wu, *J. Phys. G* **38**, 115004 (2011).
- [34] V. Skokov, B. Friman, and K. Redlich, *Phys. Rev. C* **83**, 054904 (2011).
- [35] Z. Li (for the STAR Collaboration), *Acta Phys. Pol. B Proc.* **6**, 445 (2013).
- [36] M. Bleicher *et al.*, *J. Phys. G* **25**, 1859 (1999).
- [37] J. G. Skellam, *J. R. Stat. Soc.* **109**, 296 (1946).
- [38] P. Braun-Munzinger, B. Friman, F. Karsch, K. Redlich, and V. Skokov, *Nucl. Phys. A* **880**, 48 (2012).
- [39] D. McDonald (for the STAR Collaboration), *Nucl. Phys. A* **904-905**, 907c (2013).
- [40] W. Busza and A. S. Goldhaber, *Phys. Lett. B* **139**, 235 (1984).
- [41] L. Adamczyk *et al.* (STAR Collaboration), [arXiv:1309.5681](https://arxiv.org/abs/1309.5681).
- [42] R. V. Gavai and S. Gupta, *Phys. Lett. B* **696**, 459 (2011).
- [43] X. Pan, L. Chen, X. S. Chen, and Y. Wu, *Nucl. Phys. A* **913**, 206 (2013).
- [44] X. Luo (for the STAR Collaboration), *J. Phys. Conf. Ser.* **316**, 012003 (2011).